Korean J. Chem. Eng., 37(9), 1599-1608 (2020)
DOI: 10.1007/s11814-020-0552-z

pISSN: 0256-1115
eISSN: 1975-7220

Nickel-cobalt alloy coatings prepared by electrodeposition Part I: Cathodic current efficiency, alloy composition, polarization behavior and throwing power

Rasha Muneer Al Radadi* and Magdy Ahmed Mahmoud Ibrahim,†**

*Chemistry Department, Faculty of Science, Taibah University, Al Madinah Al Mounwara, 30002 Saudi Arabia
**Chemistry Department, Faculty of Science, Ain Shams University, Abbassia, Cairo, 11566 Egypt
(*Received 17 January 2020 • Revised 29 March 2020 • Accepted 1 April 2020*)

Abstract−A systematic study was carried out to electrodeposit Ni-Co alloy coatings from a complexing acidic glycine bath on copper substrates. The effects of $[Co^{2+}]/[Ni^{2+}]$ ratio, gly concentration, pH, current density and temperature on the current efficiency, Co content in the coatings and on polarization behavior were investigated. It was found that the CCE of these baths has a wide range starting from 55% up to a maximum value of 99.3%, relying on the operating parameters and the bath constituent. However, the CCE decreased from 96.2% to 84.8% when the gly content was enhanced from 25 to 150 g/L. On the other hand, the Co content in the deposit reached 97% (wt%) at $[Co^{2+}]/[Ni^{2+}]$=0.43, i=16 mA cm^{-2}, t=10 min, T=20 °C. The codeposition of Co and Ni from acidic gly baths obeys the anomalous type of codeposition. The kinetic results indicate that the Tafel slope increased in the case of alloy deposition, while both the transfer coefficient α_c and the exchange current i^o decreased. Moreover, the obtained results indicated that increasing the Co^{2+} content in the electrolytic solution has an inhibiting impact on the kinetics of the nickel-cobalt alloy plating. The throwing power is enhanced with enhancing $[Co^{2+}]/[Ni^{2+}]$ ratios, while the addition of gly decreases it. However, the outcomes of macrothrowing power, throwing index and Wagner numbers are in excellent accord.

Keywords: Ni-Co Alloy Coatings, Cathodic Efficiency, Tafel Lines, Throwing Power, Polarization Behavior

INTRODUCTION

Nickel, cobalt and their alloy coatings are economically important in a variety of industrial applications, such as electronics, computers, automotive and devices for energy storage and for other technical applications due to their appropriate magnetic, mechanical, chemical, physical and electrocatalytic characteristics [1-9]. Recently, Ni and Co have been used as active compounds for lithium batteries and solar cells. The major advantage of using nickel and cobalt in batteries is that they deliver energy density and greater storage capacity at a reasonable cost [10-16]. Also, the electrodeposited Ni-Co alloys are applied as a reactive material for oxygen and hydrogen evolution reactions in the splitting of water, as anode electrodes for Li-battery and as catalysts for H_2O_2 decomposition [1, 17,18]. Ni-Co coatings have been achieved by electrodeposition method due to its low expense, easy to preserve the machine, uniform coating thickness, preparing high-quality alloys, the capability to handle complex geometries and low toxicity of the technique [19-22], incomparable with other coating technologies, e.g., physical and chemical vapor deposition [23,24].

The electrochemical deposition of Ni-Co alloy was extensively studied using different electrolytic solutions such as sulfate, mixed chloride-sulfate baths, sulfamate, sulfate-citrate, Watts and modified Watts bath [1,2,25-42] and from baths containing different additives [43-49]. Gly is efficacious for the electroplating processes due to its good action as a buffer and its ability to preserve the pH constant adjacent to the electrode surface [46,47,49-54]. Electrolytic plating solutions involving gly are characterized by good current efficiency and producing amorphous coatings [53]. Besides, electrolytic gly baths are more environment-favorable than classical cyanide solutions. Continuous to our successful electrodeposition of Co and Ni individually from acidic gly baths [53,54], it was ecxiting to investigate the codeposition of Ni-Co alloy coatings from these baths. Therefore, our aim was to examine the codeposition of Ni-Co coatings from acidic gly bath and to study the influence of some working circumstances, such as gly concentration, pH and temperature on the CCE%, Co percentage in the alloy, the polarization behavior and on the throwing power.

EXPERIMENTAL DETAILS

Experiments were performed from baths consisting of $CoSO_4 \cdot 7H_2O$, $NiSO_4 \cdot 6H_2O$, H_3BO_3 and NH_2CH_2COOH. The electrolytic solutions and reagents applied were prepared from analytical class chemicals and bi-distilled water. The pH was controlled by adding H_2SO_4 or KOH and was measured using a Janway 3540 pH meter. The absorption spectra of cobalt and nickel electrolytes at variable conditions were determined by UV-Visible spectrometer (GBC UV-Visible Cintra 6).

The composition of some baths examined for Ni-Co alloy codeposition is illustrated in Table 1. A Cu cathode and a Pt plate anode (2.5 cm×2.5 cm) were utilized for electrodepsoition. The deposition cell utilized was a plexiglass basin. The Cu cathode was pickled for 60 s, cleaned with distilled water, rinsed with ethanol and weighed.

†To whom correspondence should be addressed.
E-mail: imagdy1963@hotmail.com

Table 1. Composition of Ni-Co alloy baths

Baths	Concentration (g/L)				pH	Ω (mS)
	$NiSO_4$	$CoSO_4$	H_3BO_3	Glycine		
Ni-Co 1	90	10	30	100	3.63	25.2
Ni-Co 2	80	20	30	100	3.68	24.8
Ni-Co 3	75	25	30	100	3.70	25.1
Ni-Co 4	70	30	30	100	3.71	25.1
Ni-Co 5	60	40	30	100	3.74	25.0
Ni-Co 6	50	50	30	100	3.78	24.8
Ni-Co 7	40	60	30	100	3.82	25.0
Ni-Co 8	30	70	30	100	3.86	25.1

D.C. power supply unit (QJ3005A) was utilized as a direct current source. The current efficiency was calculated using the weight and compositions of the coating alloy and the quantity of electricity passed [55]. The current efficiency was calculated depending on the weight of the deposit formed at a definite condition. Therefore, it was found that the calculated current efficiency has an experimental error of ±2%. The constituent of the deposit was detected by electron dispersive X-ray spectrometry, EDX (Cambridge Scanning Company Ltd). The plating duration was 10 min.

An electrochemical station SI 1287 Solartron, was utilized for the electrochemical measurements. In polarization measurements, the cathodic potential changed linearly from its static potential (potential at zero current density) towards less noble values with a sweep rate of 10 mV s^{-1}, and the corresponding flowing current was traced as a function of potential. In all cases, triplicate experiments were carried out to ensure reproducibility. The macrothrowing power, throwing index and Wagner number were evaluated as reported previously [56-58].

RESULTS AND DISCUSSION

1. Chemistry of Ni^{2+} and Co^{2+} Complexes with Gly

Ni^{2+} and Co^{2+} ions can form soluble complexes with gly. The complex formation is found to be pH-dependent. The stability constant (K) and rate constant (k) of the different Ni and Co complexes species are listed in Table 2. The complexes of gly with Ni^{2+} are more stable than those of Co^{2+} ions [59], which are expected to produce deposits rich in cobalt. The stability of the different species was found to decrease in the following order: $NiGly^+ > NiGly_2 > CoGly^+ > CoGly_2 > NiGly_3^- > CoGly_3^-$. However, rate constants rely basically on the type of metal, whatever how much the concentration of gly is present. The rate constant values show that the Ni complexes with gly are most stable, but the Co complexes formed quicker at the same experimental conditions. Cobalt inhibits nickel due to the larger surface adsorption of the cobalt intermediate species. It is not easy to decide how gly molecules enhance the cobalt adsorption since it is impossible to anticipate the structure of the complex species created. Schwarz et al. [24] recorded that gly can form complexes with Co^{2+} or Ni^{2+} using bidentate legends via O-M-N bonds but could also do via O-M-O straight bridged bis-gly. The uncomplexed species might be more easy for electrodeposition. On the other hand, heteronuclear might be established indicating that single complexes species with both Co^{2+} and Ni^{2+} coordinated with more than one gly could also be established in the electrolyte.

Table 2. Stability (K) and rate (k) constants of glycine complexes

Species	Log K[a]	Log k[b]
$NiGly^+$	5.69	4.61
$NiGly_2$	4.83	4.75
$NiGly_3^-$	3.48	4.63
$CoGly^+$	4.51	6.18
$CoGly_2$	3.75	6.30
$CoGly_3^-$	2.23	5.90

[a]From Ref. [63]
[b]From Ref. [64]

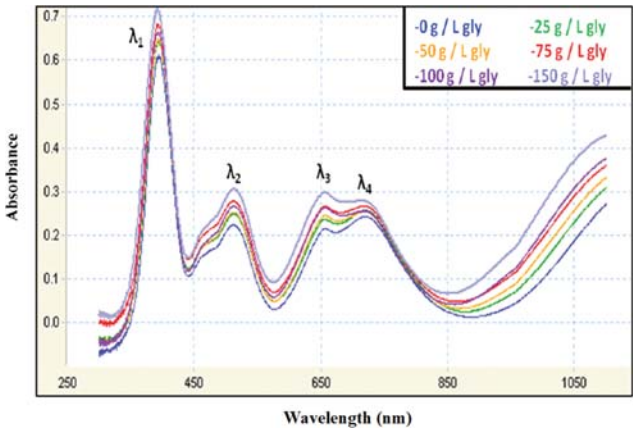

Fig. 1. Effect of gly concentration on absorption spectra for solutions containing 100 g/L $NiSO_4$, 100 g/L $CoSO_4$, 30 g/L H_3BO_3 with different gly concentrations.

2. Absorption Spectra

Figs. 1-4 show the electronic absorption spectra of Ni^{2+}, Co^{2+} and their solutions at different gly concentrations, $[Co^{2+}]/[Ni^{2+}]$ ratios, and pH. The measurements were performed in the wavelength range from 300-1,100 nm. Fig. 1 explores the effect of gly concen-

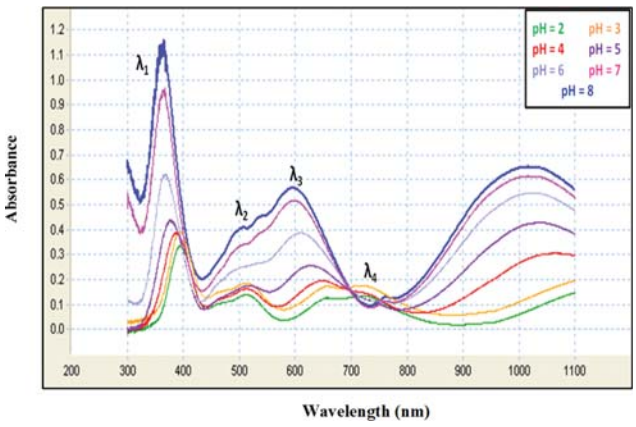

Fig. 2. Absorption spectra for solutions containing 100 g/L $NiSO_4$, 100 g/L $CoSO_4$, 30 g/L H_3BO_3 and 100 g/L gly at different pH.

trations (25-150 g/L) as a complexing agent on the absorption spectra of Ni^{2+} and Co^{2+} solutions. The spectra show four peaks at 393, 512, 655 and 720 nm, due to Co^{2+} and Ni^{2+} complexes, respectively. The data reveals no change in wavelength with a slight increase in the intensity of all peaks. The color of the electrolyte changed gradually to be darker with increasing gly concentration, suggesting the increase in the amount of gly complexes with Ni^{2+} and Co^{2+} ions.

Fig. 2 displays the influence of pH (pH 2.0-8.0) on the absorption spectrum. The absorption spectrum exhibits four peaks at λ_1= 393 nm (all pH), λ_2=512 nm (pH=2.0-5.0), λ_3=655 nm (pH=4.0-8.0) and λ_4=720 nm (pH=2.0-3.0), respectively. The intensity of bands increases with increasing pH in all peaks. The wavelength for λ_1 and λ_3 shifts toward the shorter wavelength region with increasing pH from 2 to 8. This indicates that, as the pH becomes high, the complex has a high probability to exist.

The effect of $[Co^{2+}]/[Ni^{2+}]$ ratios in the bath on the absorption spectra is given in Fig. 3. The enhancement of this ratio decreases the intensity of λ_1, λ_3 and λ_4 due to the decrease in Ni^{2+} ions in the solution. Conversely, increasing this ratio increases the intensity of λ_2. These results could be due to the increase of Co^{2+} ions in the solution.

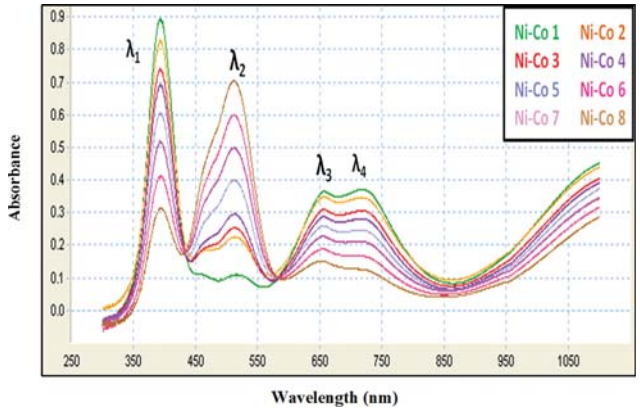

Fig. 3. Effect of $[Co^{2+}]/[Ni^{2+}]$ ratio on the absorption spectra for solutions containing 30 g/L H_3BO_3 and 100 g/L gly.

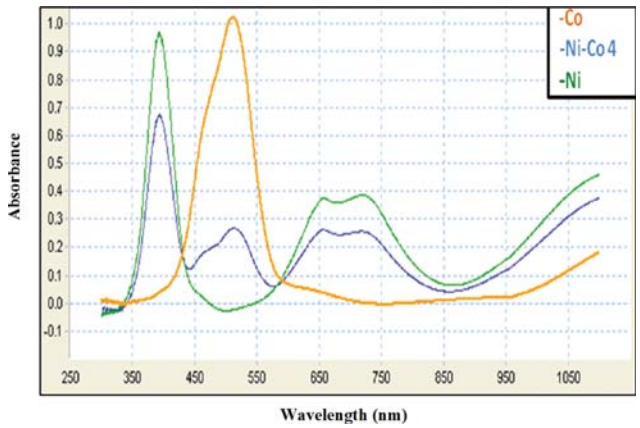

Fig. 4. Absorption spectra for Ni^{2+}, Co^{2+} and solutions of Ni and Co containing 100 g/L $NiSO_4$, 100 g/L $CoSO_4$, 30 g/L H_3BO_3 and 100 g/L gly.

Fig. 4 explores the absorption spectra of Ni^{2+}, Co^{2+} ions individually and solution of them. The data shows a peak at 512 nm for cobalt complex, and three peaks at 393, 657 and 720 nm, respectively, for nickel complex. In a solution containing both Ni^{2+} and Co^{2+} ions, four peaks are observed as mentioned previously.

3. Cathodic Current Efficiency

The impact of bath constituent and the plating conditions on the CCE was analyzed and the data are shown in Figs. 5-9. In all the experimental results the CCE% was lower than 100% as a result of simultaneous H_2 evolution associated with the coating deposition process.

Fig. 5 depicts the effect of $[Co^{2+}]/[Ni^{2+}]$ ratios in the electrolytic solution on the CCE% for the alloy codeposition. As shown in Fig. 5, increasing this ratio has no significant change in the value of CCE%, whereas the partial efficiency of Co in the coating is enhanced at the expenditure of the partial efficiency of Ni, which nearly reduces in the same ratio. The increase in Co^{2+} ion concentration in the electrolytic solution enhances its efficiency for deposition as a result of a decline in the concentration overvoltage at the cathode.

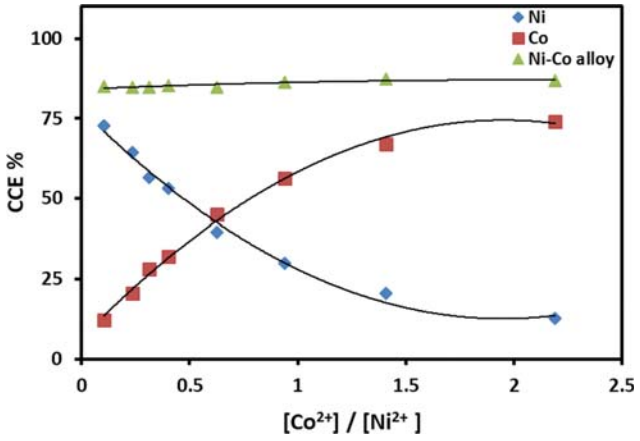

Fig. 5. Effect of $[Co^{2+}]/[Ni^{2+}]$ ratios in the bath on the CCE% of Ni-Co alloy deposition from bath containing 30 g/L H_3BO_3, 100 g/L gly (i=16 mA cm^{-2}, t=10 min, T=20 °C).

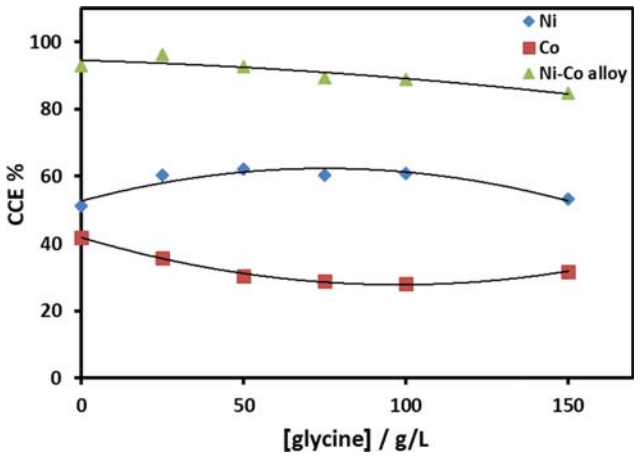

Fig. 6. Effect of gly concentrations on the CCE% during Ni-Co alloy deposition from bath containing 70 g/L $NiSO_4$, 30 g/L $CoSO_4$ 30 g/L H_3BO_3 (i=16 mA cm^{-2}, t=10 min, T=20 °C).

On the other hand, increasing gly concentration has a slight decreasing influence on CCE% for coating deposition as shown in Fig. 6. For example, the CCE decreases from 96.2% to 84.8% when the gly concentration is enhanced from 25.0 to 150.0 g/L. This reducing effect might be assigned to the fact that enhancing the concentration of gly enhances the complex ions concentration and reduces the free Co^{2+} and Ni^{2+} ions concentrations, leading to enhancing the overpotential and decreasing the CCE%. Similar behavior was recorded during the codeposition of Co-Cu alloy and Zn-Co-Cu alloy from an alkaline glycinate bath [60,61].

Fig. 7 represents the impact of the applied current density (6.7-33.0 mA cm^{-2}) on the CCE of alloy codeposition. It was found that the CCE of alloy deposition increased slightly to a maximum value of 99.3% at 20 mA cm^{-2} and then decreased slightly to 87.9% at 33 mA cm^{-2}. The partial current efficiency of Ni-plating increased, while that of cobalt decreased with enhancing the current density. The decline in the CCE of alloy codeposition at high current densities might be assigned to enhancement in the efficacy of hydrogen evolution and the decline in the efficacy of cobalt reduction.

The pH value of the bath (pH 3.5-pH 8.2) affects greatly the CCE of the alloy codeposition. The CCE decreases gradually from 89.0 to 58.0 when the pH changes from pH 3.5 to 8.2 (except at pH 3.5) as shown in Fig. 8. This could be ascribed to the high stability of the complexes formed by increasing the pH of the electrolytic solution. Moreover, increasing the pH of the bath diminishes the contribution of H_2 reaction, since the H_2 overpotential increases significantly with increasing the pH.

On the other hand, Fig. 9 shows how CCE of Ni-Co alloy codeposition is decreased significantly by raising the bath temperature from 20 to 60 °C. This appears to be the result of the enhancement in the partial efficacy of H_2 evolution and a reduction in the partial current efficacy of Ni deposition [62]. High efficacy at ambient temperature might be proposed as a significant manufacturing benefit for Ni-Co alloy codeposition from the present gly acidic bath. Similar behavior of decreasing CCE with increasing temperature was observed during Sn-Ni deposition from acidic chloride bath [62]. Generally speaking, it was found that the CCE of these baths had a wide range starting from 55% up to a maximum

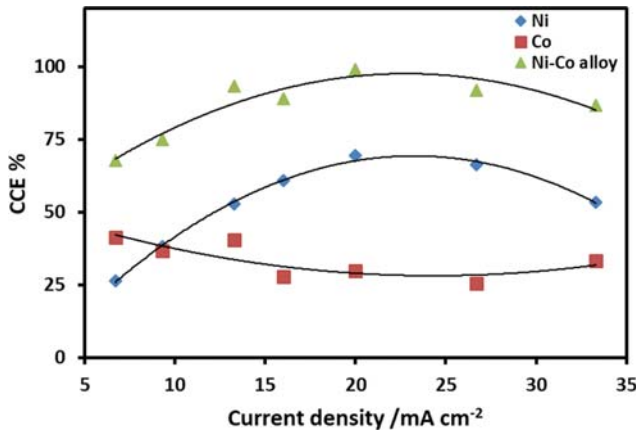

Fig. 7. Effect of current density on the CCE% during Ni-Co alloy deposition from bath containing 70 g/L $NiSO_4$, 30 g/L $CoSO_4$, 30 g/L H_3BO_3 and 100 g/L gly (t=10 min, T=20 °C).

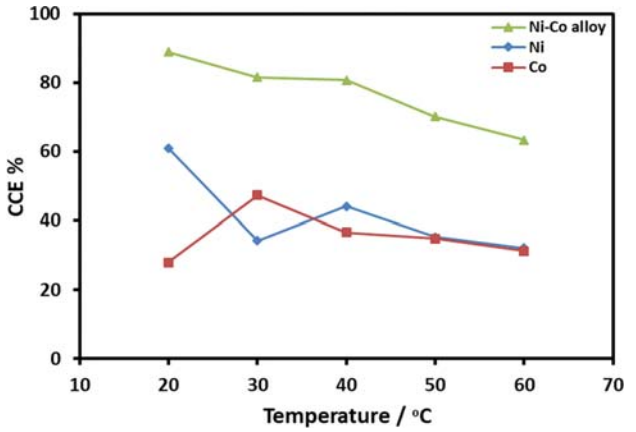

Fig. 9. Effect of bath temperature on the CCE% during Ni-Co alloy deposition from bath containing 70 g/L $NiSO_4$, 30 g/L $CoSO_4$, 30 g/L H_3BO_3 and 100 g/L gly (i=16 mA cm^{-2}, t=10 min).

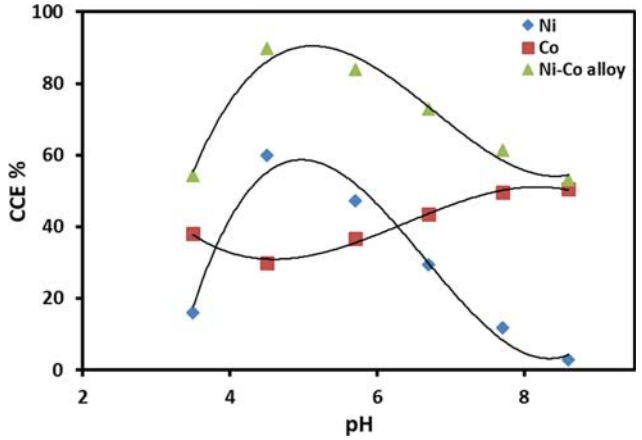

Fig. 8. Effect of pH on the CCE% during Ni-Co alloy deposition from bath containing 70 g/L $NiSO_4$, 30 g/L $CoSO_4$, 30 g/L H_3BO_3 and 100 g/L gly (i=16 mA cm^{-2}, t=10 min, T=20 °C).

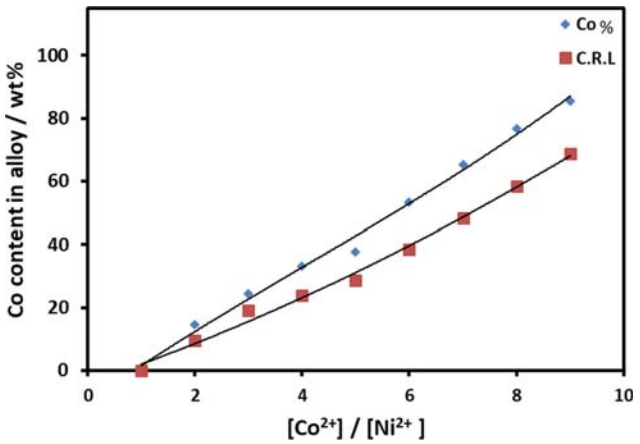

Fig. 10. The effect of $[Co^{2+}]/[Ni^{2+}]$ ratios on the cobalt content in the alloy from bath containing 30 g/L H_3BO_3, 100 g/L gly (i=16 mA cm^{-2}, t=10 min, T=20 °C).

value of 99.3%, relying on the operating parameters and the bath constituent which could be considered higher than other baths [2].

4. The Composition of the Ni-Co Coatings

Figs. 10-14 explore the elemental analysis of Ni-Co alloys at different deposition conditions. The composition reference line (C.R.L.) is defined as:

$$\text{C.R.L.} = \left(\frac{[Co^{2+}]}{[Co^{2+}]+[Ni^{2+}]}\right)\times 100 \quad (1)$$

where $[Co^{2+}]$ and $[Ni^{2+}]$ are the content of Co^{2+} and Ni^{2+} ions in the electrolytic solution. It was found that the Co content (the less noble element) in the alloy was greater than its content in the solution and it lay over the C.R.L. These data mean that cobalt is the more easily depositable element as predicted from the polarization curves. Thus, the deposition of cobalt and nickel together from the gly electrolytic solution obeys the anomalous kind of codeposition.

Fig. 10 reveals the relationship between $[Co^{2+}]/[Ni^{2+}]$ ratios in the electrolytic solution and the cobalt content of deposited alloy. It is observed that at all $[Co^{2+}]/[Ni^{2+}]$ ratios in the electrolytic solution, the cobalt content are always higher than its content in the bath. This means that the rate of reduction of Co^{2+} ions seems to be greater than that of Ni^{2+} ions, i.e., the reduction of Ni^{2+} ions (more noble element) is prohibited while the reduction of Co^{2+} ions (less noble element) is promoted, as expected in anomalous codeposition. Similar results were reported during Ni-Co deposition from different baths [27,30].

Fig. 11 depicts the relationship between the gly concentration and the cobalt percentage in the deposit. Investigation of the results reveals that the existence of gly in the electrolytic solution does not inhibit the anomalous behavior of deposition. Indeed, the Co content is always above the C.R.L., whatever the concentration of gly in the electrolyte. The slight decrease in the Co percentage in the coating in the existence of gly could be attributable to the enhancement in the stability of Co^{2+}- gly complex species and consequent prohibition of cobalt deposition at the expense of Ni and hydrogen reduction.

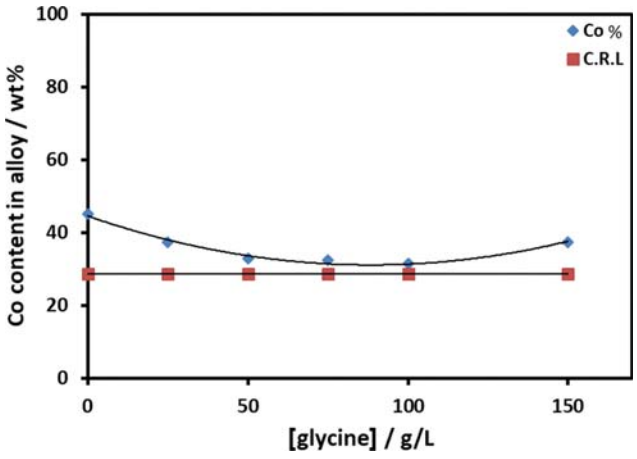

Fig. 11. Effect of gly concentrations on cobalt content of alloy during Ni-Co deposition from bath containing 30 g/L $CoSO_4$, 70 g/L $NiSO_4$, 30 g/L H_3BO_3 (i=16 mA cm^{-2}, t=10 min, T=20 °C).

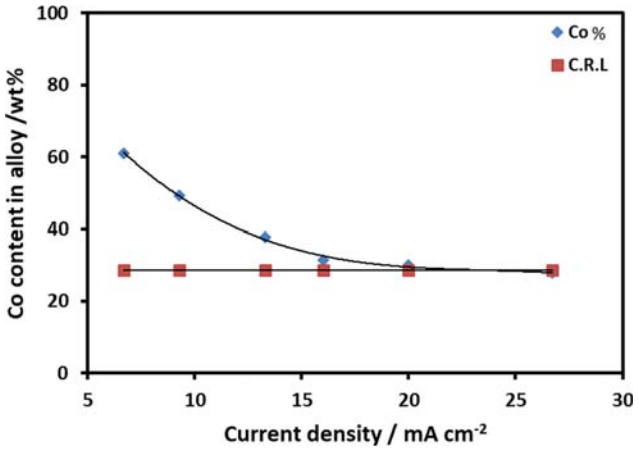

Fig. 12. Effect of current density on cobalt content of alloy during Ni-Co deposition from bath containing 30 g/L $CoSO_4$, 70 g/L $NiSO_4$, 30 g/L H_3BO_3 and 100 g/L gly (t=10 min, T=20 °C).

Fig. 12 illustrates the impact of current density on the Co percentage in the deposit. The Co percentage is reduced with enhancing current density. However, at current ≥20 mA cm^{-2}, the Co content becomes equal to that in the bath. A similar trend of decreasing Co content with enhancing current was recorded during Ni-Co deposition from sulfamate bath [39]. Nonetheless, the decline in the Co content, the less favorable depositable element, with enhancing the current is another affirmation that the coating deposition is of anomalous codeposition kind.

Fig. 13 shows the effect of pH on the cobalt percentage of the coating. The appearance of a minimum in the graph indicates that the value of pH in the existence of complexing agents could be considered as an important factor. It was found that, except at pH 3.0, which has Co content of 70 wt%, increasing pH above 4, increases the Co content greatly. Therefore, increasing the pH from 4.0 to 8.0 enhances dramatically the Co percentage in the coating from 33 to 95 wt%. The highest Co content (95 wt%) was revealed in the alloy coatings produced at pH 8.0. This means that the Co-rich

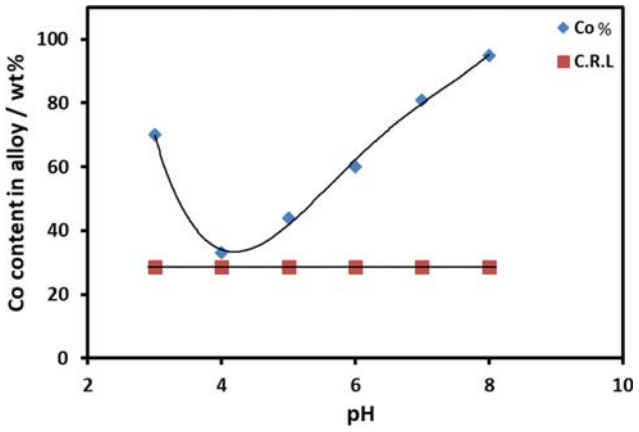

Fig. 13. Effect of pH on cobalt content of alloy during Ni-Co deposition from bath containing 30 g/L $CoSO_4$, 70 g/L $NiSO_4$, 30 g/L H_3BO_3 and 100 g/L gly (i=16 mA cm^{-2}, t=10 min, T=20 °C).

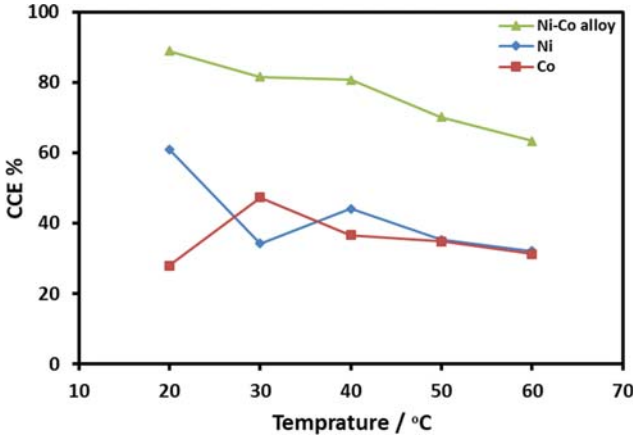

Fig. 14. Effect of temperature on cobalt content of alloy during Ni-Co deposition from bath containing 30 g/L $CoSO_4$, 70 g/L $NiSO_4$, 30 g/L H_3BO_3 and 100 g/L gly (i=16 mA cm^{-2}, t=10 min).

Ni-Co alloy could be easily prepared at the highest pH studied (pH 8.0). This is attributed to the fact that Ni^{2+} ions complexation with gly is higher than Co^{2+} ions with gly, which could be described by matching the complexation constants of Co^{2+} and Ni^{2+} glycinate complexes [63]. The numerous aqua complexes of Co^{2+} at this pH also assists to augment the coatings in cobalt. Both impacts, metal complexation and anomalous codeposition, support the deposition of Co over the Ni one. It is also interesting to observe that at all pH values the Co content is always higher than its C.R.L., as mentioned before.

Enhancement of electrolyte temperature from 20 to 60 °C enhances the Co percentage in the coating from 30 to 50 wt% as shown in Fig. 14. This means that the anomalous phenomena are increased by increasing the bath temperature.

5. Polarization Behavior

The linear polarization curves of nickel-cobalt codeposition onto copper substrates were measured at various deposition conditions and the data are given in Figs. 15-19. Fig. 15 explores the polarization behavior of the electrochemical deposition of nickel, cobalt and nickel-cobalt alloy under comparable operating conditions. The i-E curve of nickel deposition lies at considerably nobler potentials than that of Co, reflecting that nickel is the more noble element. Furthermore, the i-E curve for Ni-Co deposition lies between those of the parent elements. The codeposition allows the less noble element (cobalt) to deposit at more positive potentials and causes the more noble element (nickel) to reduce at more negative potentials.

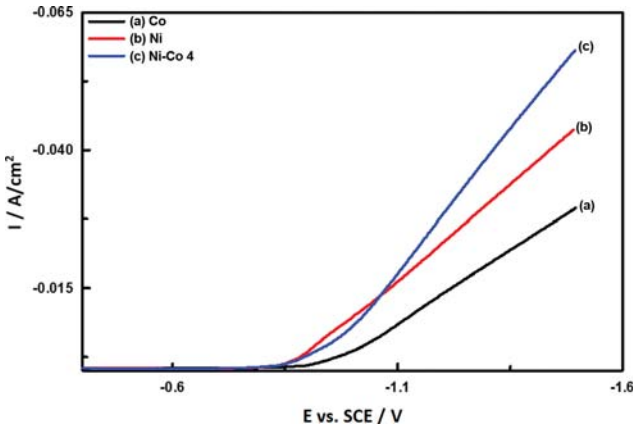

Fig. 15. Polarization behavior for individual Ni, Co and for Ni-Co alloy codeposition, scan rate=10 mV s^{-1}.

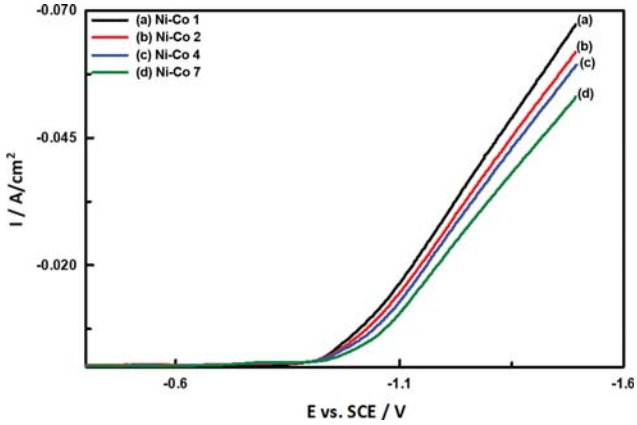

Fig. 16. Polarization behavior during Ni-Co alloy deposition at different $[Co^{2+}]/[Ni^{2+}]$ ratios in the bath, scan rate=10 mV s^{-1}.

The polarization curves recorded using different $[Co^{2+}]/[Ni^{2+}]$ ratios in the bath are illustrated in Fig. 16. It is observed that increasing this ratio moves the polarization to the less noble potential values due to the enhancement in concentration polarization, indicating that the increase in this ratio inhibits the alloy deposition.

Fig. 17 shows that the i-E curves of nickel-cobalt coating deposition enhance with increasing the gly concentration. The overpotential is enhanced due to a decline in the free Co^{2+} and Ni^{2+} ions concentrations when the complexing agent content is enhanced. This is largely assigned to the enhanced stability of Ni and Co-gly complexes. Indeed, the deposition from the complexed species is not so simple as the deposition from the free Co^{2+} and Ni^{2+} ions. Similar behavior was recorded during the codeposition of Co-Cu alloy and Zn-Co-Cu coating from alkaline glycinate baths [60,61].

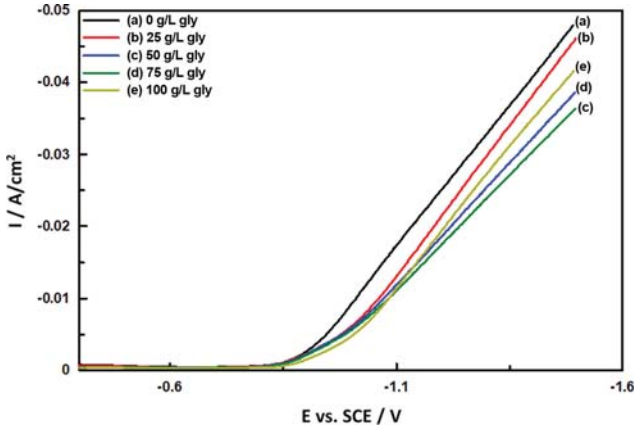

Fig. 17. Polarization behavior during Ni-Co alloy deposition from bath containing 100 g/L $NiSO_4$, 30 g/L $CoSO_4$, 30 g/L H_3BO_3 at different gly concentration, scan rate=10 mV s^{-1}.

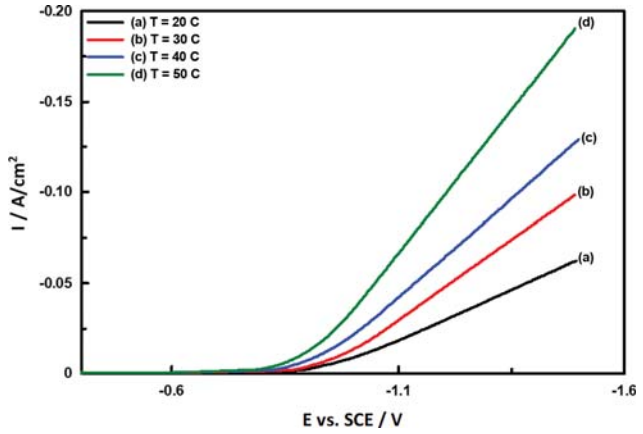

Fig. 18. Polarization behavior during Ni-Co alloy deposition from bath containing 100 g/L $NiSO_4$, 30 g/L $CoSO_4$, 30 g/L H_3BO_3 and 100 g/L gly at different temperature, scan rate=10 mV s^{-1}.

The impact of temperature on the i-E curve of Ni-Co alloy is displayed in Fig. 18. Raising the electrolyte temperature significantly shifts the i-E curve to the less negative potential. It seems that an increase in temperature generally favors the complex ion dissociation. Thus, the concentration of the free ions would increase and lead to a decrease in the reduction of overpotential.

The impact of pH value on the polarization curves of nickel-cobalt coating is given in Fig. 19(A), (B). It was found that the polarization of the coating deposition is significantly pH-dependent, and the polarization is moved to less noble potentials as the pH of the electrolyte is enhanced (pH 2.2 to pH 5.2). This trend may be due to the stability of the complexes formed and the stability enhance with increasing pH. However, in the pH range from 6.2 to 8.1 interference between the polarization curves takes place.

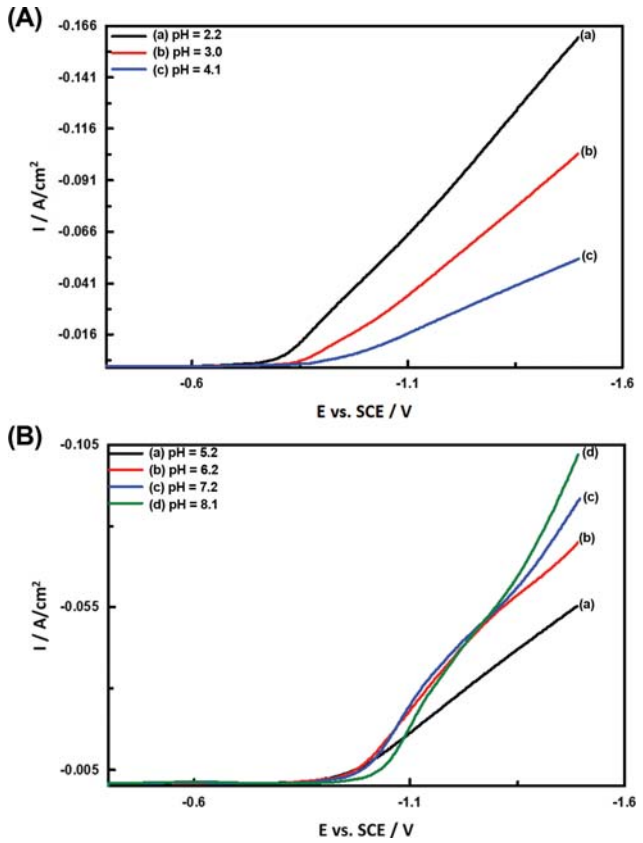

Fig. 19. Polarization behavior during Ni-Co alloy deposition from bath containing 100 g/L $NiSO_4$, 30 g/L $CoSO_4$, 30 g/L H_3BO_3 and 100 g/L gly at different pH, scan rate=10 mV s^{-1}.

6. Tafel and Electrokinetic Parameters

To examine the impact of bath constituents and the working criteria on the kinetics of the electrode, Tafel constants were deduced from their i-E curves (Figs. 15-19). Tafel slope describes how responsive the current is to the applied potential. A high Tafel slope shows that the bandgap energy is high, which leads to a high overpotential due to the large amount of energy required to achieve activity and vice versa. Also, the values of the electrokinetic criteria, i^o (exchange current densities), α_c (the transfer coefficient), are evaluated and given in Table 3. The transfer coefficient α_c is given by Eq. (2):

$$\alpha_c = -(RT/nF)(d\ln|i_c|/dE) \quad (2)$$

where i_c is the cathodic current density, E is the potential, R, T and F have their accustomed magnitudes [65]. The results in Table 3 show that the Tafel slope increased in the case of alloy deposition

Table 3. Tafel slope and kinetic parameters at different conditions for Ni-Co alloy codeposition

Variable	i_o (A cm^{-2})	α_c	$-b_c$ (mV $decade^{-1}$)
Co	0.120	0.89	333
Ni	0.180	0.08	376
Ni-Co 4	0.073	0.05	580
Alloy			
Ni-Co 1	0.201	0.09	342
Ni-Co 2	0.188	0.09	337
Ni-Co 4	0.175	0.09	331
Ni-Co 7	0.192	0.09	299
[glycine]/g/L			
0	0.102	0.06	496
25	0.117	0.07	409
50	0.123	0.08	382
100	0.183	0.09	318
pH			
2.2	0.217	0.04	735
3.0	0.183	0.06	532
4.1	0.117	0.07	448
5.2	0.156	0.08	388
6.2	0.248	0.08	356
7.2	0.407	0.99	297
8.1	1.386	0.16	189
Temp./°C			
20	0.183	0.09	337
30	0.375	0.09	340
40	0.376	0.07	400
60	0.379	0.06	517

in comparison with the individual deposition of Co^{2+} or Ni^{2+} ions, while both the transfer coefficient α_c and i^o are significantly decreased. On the other hand, i^o decreased with enhancing $[Co^{2+}]/[Ni^{2+}]$ ratios in the bath. The obtained results pointed out that enhancing Co percentage in the electrolytic solution has a prohibiting impact on the kinetics of Ni-Co reduction, as shown by the decline of i^o. The surface of the electrode is more active if i^o is high. Thus, the higher the i^o, the more current is produced at any overpotential. Generally, i^o declines when the reaction is prohibited [66]. Therefore, Co^{2+} ions inhibit the rate of Ni^{2+} ion transferthrough the EDL. This data is in very good accord with the theories of anomalous deposition which claims that Co^{2+} retards the reduction of Ni^{2+} ions. On the other hand, the inclusion of gly into the plating baths enhances i_o and decreases the Tafel slope, while the transfer coefficient is slightly increased. The impact of pH was tested and the data are in Table 3. The data show that, at pH 2.2- 4.1, i_o decreases as well as the Tafel slope, while α_c increases. However, at pH between 5.2-8.1, i_o increases but the Tafel slopes decrease. However, enhancing the solution temperature from 20 to 30 °C increases i_o and then, with further increase in temperature, i_o value tends to be constant, while the Tafel slope increases and the α_c decreases (Table 3).

7. Macrothrowing Power of the Electrolytic Solutions

A look at the literature displays a shortage in the throwing power (TP) data of Ni-Co alloy electrodeposited from different electrolytic solutions [1,6,28,32]. The TP values of the Ni-Co electrolytic solutions determined by Field's formulation utilizing a Haring-Blum cell under various deposition criteria are in Table 4. Examination of the data in Table 4 shows that the TP of Ni-Co electrolytic solution increases with enhancing $[Co^{2+}]/[Ni^{2+}]$ ratios in the bath. For example, increasing this ratio from 0.25 to 1.5 increases greatly the TP% from −9.52 to 0. This might be ascribed to the increase in polarization with enhancing this ratio as shown in Fig. 16. Furthermore, the gly addition to the Ni-Co electrolytic solution lowers the TP. This decreasing effect in TP enhances with increasing gly concentration as shown in Table 4. It is interesting that the addition of gly enhances the TP for cobalt bath since it leads to an increase in the polarization [53]. However, it decreases greatly the TP for Ni bath because of the depolarizing effect [54]. However, enhancing the current density decreases the TP of the Ni-Co plating bath.

Some of the uncertainty correlated with the application of the hypothesis of TP can be determined by the application of throwing index TI, which is achieved by drawing the metal distribution ratio M against the linear current distribution ratio L. The reverse of the slope of the line acquired is the throwing index and symbolizes a direct assessment for the electrolytic solution TP. Representative plots between M and L (1 : 1-1 : 5) are specified in Figs. 20-22. The significant numbers of TP and TI shown in Table 4 disclose that the specified TI alter in a side by side manner to those determined for TP.

Wagner number Wa [67], given by Eq. (3), represents the quotient of the polarization resistance to the solution resistance. The Wagner number is given by:

$$Wa=(k/X)\,(d\eta/di) \quad (3)$$

Table 4. Throwing power, throwing index and Wagner number for Ni-Co alloy deposition

Variable	TP	TI	Wa
Baths			
Ni-Co 2	−9.52	0.75	0.76
Ni-Co 4	−6.29	0.77	0.77
Ni-Co 7	0.00	0.89	0.85
[glycine]/g/L			
0.0	0.00	0.98	1.25
50	−9.09	0.89	1.11
75	−11.11	0.77	1.01
100	−14.89	0.75	0.79
Current density/mA cm^{-2}			
6.7	−3.70	0.88	-
9.3	−4.76	0.82	-
16	−6.29	0.78	-
26.7	−15.03	0.72	-

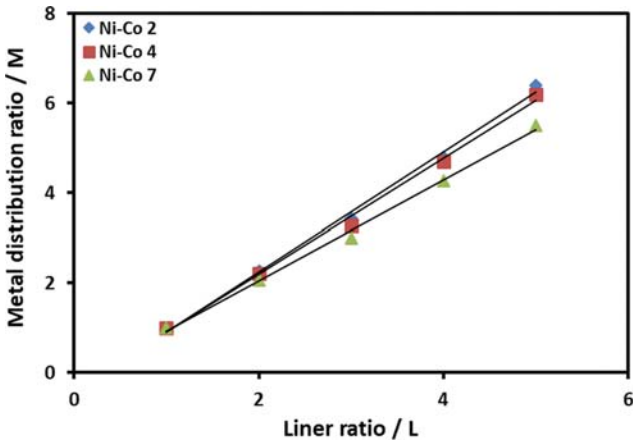

Fig. 20. Metal distribution ratio M vs. the linear ratio L at different $[Co^{2+}]/[Ni^{2+}]$ ratios in the presence of 30 g/L H_3BO_3 and 100 g/L gly (i=16 mA cm^{-2}, t=10 min, T=20 °C).

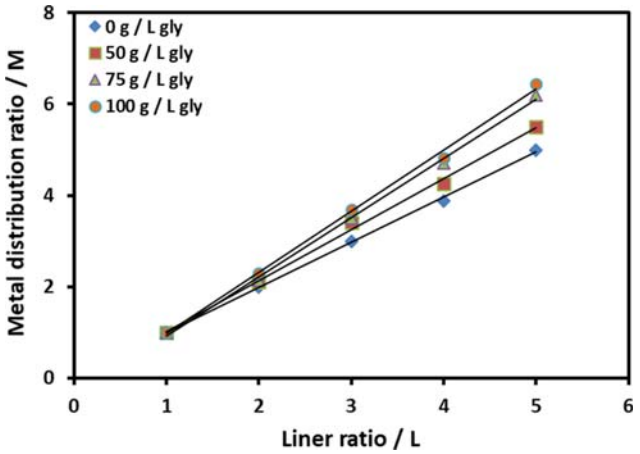

Fig. 21. Metal distribution ratio M vs. the linear ratio L at different gly concentration in the presence of 100 g/L $CoSO_4$, 100 g/L $NiSO_4$, 30 g/L H_3BO_3 (i=16 mA cm^{-2}, t=10 min, T=20 °C).

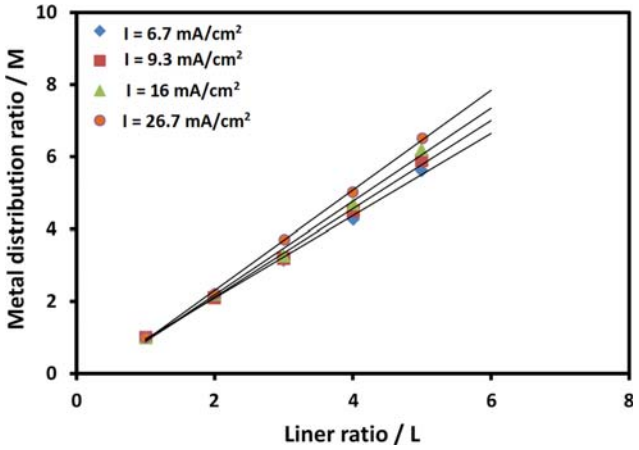

Fig. 22. Metal distribution ratio M vs. the linear ratio L at different current density in the presence of 100 g/L $CoSO_4$, 100 g/L $NiSO_4$, 30 g/L H_3BO_3 and 100 g/L gly (t=10 min, T=20 °C).

where k is the conductivity of the electrolytic solution, X is the electrode length (3.0 cm) and ($d\eta$/di) is the slope of the i-E curve. The current distribution is more uniform if X is small and k of the solution is large, and the slope of the i-E curve is large. The Wa calculated for different baths is given in Table 4. The data affirm that the current distribution is more symmetric as Wa is enhanced. The results of TP, TI and Wa are in excellent accord. The more symmetric the current distribution, the better Wa and thus the better the TP and the TI.

CONCLUSIONS

Nickel-cobalt alloy coatings were successfully codeposited from complexing acidic gly baths on a copper substrate. The CCE of these baths had a wide range starting from 55% up to a maximum value of 99.3%, relying on the operating parameters and the bath constituent. However, the CCE decreased from 96.2% to 84.8% when the gly concentration was increased from 25.0 to 150 g/L. The Co content in the deposit reached 97 (wt%) at $[Co^{2+}]/[Ni^{2+}]$=0.43, i= 16 mA cm^{-2}, t=10 min, T=20 °C. The codeposition of cobalt and nickel from gly electrolytic solution obeys the anomalous kind of codeposition. The cathodic polarization curves of Ni-Co alloy coatings increased with enhancing either the $[Co^{2+}]/[Ni^{2+}]$ ratios, pH or increasing gly concentration while it decreased with temperature. The kinetic results indicate that the Tafel slope increased in the case of alloy deposition, while both the transfer coefficient α_c and the exchange current i^o decreased. Moreover, from the obtained results, enhancing Co percentage in the electrolytic solution had an inhibiting impact on the kinetics of the Ni-Co deposit. The throwing power of Ni-Co bath was enhanced with enhancing $[Co^{2+}]/[Ni^{2+}]$ ratios in the electrolytic solution, while the gly addition to the Ni-Co plating solution lowered the TP.

REFERENCES

1. T. Mahalingam, K. Sundaram, S. Velumani, M. Raja, S. Thanikaikarasan, Y. D. Kim and R. Asomoza, *Adv. Mater. Res.*, **68**, 52 (2009).
2. L. Tian, J. Xu and S. Xiao, *Vacuum*, **86**, 27 (2011).
3. G. Carac and A. Ispas, *J. Solid State Electrochem.*, **16**, 3457 (2012).
4. B. Bakhit and A. Akbari, *J. Coat. Technol. Res.*, **10**(2), 285 (2013).
5. M. C. Esteves, P. T. A. Sumodjo and E. J. Podlaha, *Electrochim. Acta*, **56**, 9082 (2011).
6. A. Karimzadeha, M. Aliofkhazraeia and F. C. Walsh, *Surf. Coat. Technol.*, **372**, 463 (2019).
7. R. Abdel-Karim, M. Ramadan and S. M. El-Raghy, *J. Nanomaterials*, **2018**, 13 (2018).
8. S. Vasefi and M. Parrari, *Korean J. Chem. Eng.*, **27**(2), 422 (2010).
9. H. Park, K. M. Kim, H. Kim, D.-K. Kim, Y. S. Won and S.-K. Kim, *Korean J. Chem. Eng.*, **35**(7) 1547 (2018).
10. M.-G. Jeong, K. Zhuo, S. Cherevko and C.-H. Chung, *Korean J. Chem. Eng.*, **29**(12) 1802 (2012).
11. K.-I. Jang, E. Hang and J. H. Kim, *Korean J. Chem. Eng.*, **30**(3), 620 (2013).
12. Y. He, S. Hwang, D. A. Cullen, M. A. Uddin, L. Langhorst, B. Li, S. Karakalos, A. Kropf, E. C. Wegener, J. Sokolowski, M. Chen, D. Myers, D. Su, K. L. More, G. Wang, S. Litster and G. Wu, *Energy Environ. Sci.*, **12**, 250 (2019).
13. A. Dokouzis, F. Bella, K. Theodosiou, C. Gerbaldi and G. Leftheriotis, *Mater. Today Energy*, **15**, 100365 (2020).
14. A. Kamppinen, K. Aitola, A. Poskela, K. Miettunen and P. D. Lund, *Electrochim. Acta*, **335**, 135652 (2020).
15. B. Baptayev, A. Aukenova, D. Mustazheb and M. P. Balanay, *J. Photochem. Photobiol. A*, **383**, 111977 (2019).
16. N. Nita, F. Wu, J. T. Lee and G. Yushin, *Mater. Today*, **18**(5), 252 (2015).
17. V. D. Jovic, B. M. Jovic, M. G. Pavlovic and V. Maksimovic, *J. Solid State Electrochem.*, **10**, 959 (2006).
18. S. G. Kandalkar, H.-M. Lee, S. H. Seo, K. Lee and C.-K. Kim, *Korean J. Chem. Eng.*, **28**(6), 1464 (2011).
19. J. Vijayakumar, S. Mohan, S. A. Kumar, S. R. Suseendiran and S. Pavithra, *Int. J. Hydrogen Energy*, **38**, 10208 (2013).
20. Y. H. You, C. D. Gu, X. L. Wang and J. P. Tu, *Surf. Coat. Technol.*, **206**, 3632 (2012).
21. J.-m. Li, C. Cai, L.-x. Song, J.-f. Li, Z. Zhang, M.-z. Xue and Y.-g. Liu, *Trans. Nonferrous Met. Soc. China*, **23**, 2300 (2013).
22. L. Shi, C. F. Sun, P. Gao, F. Zhou and W. M. Liu, *Surf. Coat. Technol.*, **200**, 4870 (2006).
23. A. N. Correia and S. A. S. Machado, *J. Appl. Electrochem.*, **33**, 367 (2003).
24. M. Schwartz, N. V. Myung and K. Nobe, *J. Electrochem. Soc.*, **151**(7), C468 (2004).
25. I. Z. Rahman, M. V. Khaddem-Mousavi, A. A. Gandhi, T. F. Lynch and M. A. Rahman, *J. Phys. Conference Series*, **61**, 523 (2007).
26. C. A. Harper, *Electronic materials and processes handbook*, McGraw Hill Professional, 1.6, New York NY (2003).
27. C. Lupi, A. Dellera, M. Pasquali and P. Imperatori, *Surf. Coat. Technol.*, **205**, 5394 (2011).
28. L. Wang, Y. Gao, Q. Xue, H. Liu and T. Xu, *Appl. Surf. Sci.*, **242**, 326 (2005).
29. O. Ergenema, K. M. Sivaraman, S. Pane, E. Pellicer, A. Telekic, A. M. Hirt, M. D. Baro and B. J. Nelson, *Electrochem. Acta*, **56**, 1399 (2011).
30. D. Golodnitsky, Y. Rosenberg and A. Ulus, *Electrochim. Acta*, **47**, 2707 (2002).

31. Y. Yu-Fang, D. Bin and W. Zhao-Hui, *Adv. Chem. Eng. Sci.*, **1**, 27 (2011).
32. J. Vazquez-Arenas and M. Pritzker, *J. Solid State Electrochem.*, **17**, 419 (2013).
33. E. Gomez, S. Pane and E. Valles, *Electrochim. Acta*, **51**, 146 (2005).
34. H. El-Feky, M. Negem, S. Roy, N. Helal and A. Baraka, *Sci. China. Chem.*, **56**(10), 1446 (2013).
35. S. Goldbach, R. De Kermadec and F. Lapicque, *J. Appl. Electrochem.*, **30**, 277 (2000).
36. A. Karpuz, H. Kockar and M. Alper, *Appl. Surf. Sci.*, **257**, 3632 (2011).
37. A. Karpuz, H. Kockar, M. Alper, O. Karaagac and M. Haciismailoglu, *Appl. Surf. Sci.*, **258**, 4005 (2012).
38. A. Karpuz, H. Kockar and M. Alper, *J. Mater. Sci. Mater. Electron.*, **24**, 3376 (2013).
39. D. Golodnitsky, N. V. Gudin and G. A. Volyanuk, *J. Electrochem. Soc.*, **147**(11), 4156 (2000).
40. J. Idris, C. Christian and E. Gaius, *J. Nano Mat.*, **2013**, 1 (2013).
41. S. Hassani, K. Raeissi, M. Azzi, D. Li, M. A. Golozar and J. A. Szpunar, *Corros. Sci.*, **51**, 2371 (2009).
42. B. Bakhit and A. Akbari, *J. Coat. Technol. Res.*, **10**(2), 285 (2013).
43. S. Hassani, K. Raeissi and M. A. Golozar, *J. Appl. Electrochem.*, **38**, 689 (2008).
44. K. R. Marikkannu, G. P. Kalaignan and T. Vasudevan, *J. Alloys Compd.*, **438**, 332 (2007).
45. E. Pellicer, S. Pane, K. M. Sivaraman, O. Ergeneman, S. Surinach, M. D. Baro, B. j. Nelson and J. Sort, *Mater. Chem. Phys.*, **130**, 1380 (2011).
46. O. A. Taranina, N. V. Evreinova, I. A. Shoshina, V. N. Naraev and K. I. Tikhonov, *Russ. J. Appl. Chem.*, **83**(1), 58 (2010).
47. Y. Zhang, L. Feng and W. Qiu, *J. Mater. Sci.*, **54**, 9507 (2019).
48. R. Tarozaite, A. Sudavicius, Z. Sukackiene and E. Norkus, *Trans. IMF*, **92**(3), 146 (2014).
49. M. H. Gharahcheshmeh and M. H. Sohi, *J. Appl. Electrochem.*, **40**, 1563 (2010).
50. J. C. Wei, M. Schwartz and K. Nobe, *J. Electrochem. Soc.*, **155**, D660 (2008).
51. T. Boiadjieva, D. Kovacheva, L. Lyutov and M. Monev, *J. Appl. Electrochem.*, **38**, 1435 (2008).
52. U. Lačnjevac, B. M. Jović and V. D. Jović, *J. Electrochem. Soc.*, **159**(5), D310 (2012).
53. M. A. M. Ibrahim and R. M. Al Radadi, *Mat. Chem. Phys.*, **151**, 222 (2015).
54. M. A. M. Ibrahim and R. M. Al Radadi, *Int. J. Electrochem. Sci.*, **10**, 4946 (2015).
55. A. Brenner, *Electrodeposition of alloys*, Academic Press, New York, 1 (1963).
56. M. A. M. Ibrahim and R. S. Bakdash, *Surf. Coat. Technol.*, **282**, 139 (2015).
57. M. A. M. Ibrahim and R. S. Bakdash, *Trans. IMF*, **92**(4), 218 (2014).
58. M. A. M. Ibrahim, *J. Chem. Technol. Biotechnol.*, **75**, 745 (2000).
59. R. Muri, K. Kurakane and T. Sekine, *Bull. Chem. Soc. Jpn.*, **49**, 335 (1976).
60. A. E. Mohamed, S. M. Rashwan, S. M. Abdel-Wahaab and M. M. Kamel, *J. Appl. Electrochem.*, **33**(11), 1085 (2003).
61. S. M. Rashwan, *Mater. Chem. Phys.*, **89**, 192 (2005).
62. M. A. M. Ibrahim, S. S. Abd El Rehim, M. M. El Naggar and M. A. Abbass, *J. Appl. Surf. Finish.*, **1**(4), 293 (2006).
63. R. M. Smith, A. E. Martell and R. J. Motekaitis, Critical Stability Constants of Metal Complexes Database, version 8.0, NIST, U.S. (2004).
64. G. Davies, K. Kustin and R. F. Pasternack, *Inorg. Chem.*, **8**, 1535 (1969).
65. R. Guidelli, R. G. Compton, J. M. Feliu, E. Gileadi, J. Lipkowski, W. Schmickler and S. Trasatti, *Pure Appl. Chem.*, **86**(2), 245 (2014).
66. M. Mouanga, L. Ricq, G. Douglade, J. Douglade and P. Bercot, *Surf. Coat. Technol.*, **201**, 762 (2006).
67. C. Wagner, *J. Electrochem. Soc.*, **98**, 116 (1951).